Journal of Geodesy (2020) 94:10
https://doi.org/10.1007/s00190-019-01335-w

ORIGINAL ARTICLE

On the interoperability of IGS products for precise point positioning with ambiguity resolution

Simon Banville[1] · Jianghui Geng[2] · Sylvain Loyer[3] · Stefan Schaer[4] · Tim Springer[5] · Sebastian Strasser[6]

Received: 24 May 2019 / Accepted: 9 December 2019 / Published online: 3 January 2020
© Crown 2020

Abstract
Techniques enabling precise point positioning with ambiguity resolution (PPP-AR) were developed over a decade ago. Several analysis centers of the International GNSS Service (IGS) have implemented such strategies into their software packages and are generating (experimental) PPP-AR products including satellite clock and bias corrections. While the IGS combines individual orbit and clock products as standard to provide a more reliable solution, interoperability of these new PPP-AR products must be confirmed before they can be combined. As a first step, all products are transformed into a common observable-specific representation of biases. It is then confirmed that consistency is only ensured by considering both clock and bias products simultaneously. As a consequence, the satellite clock combination process currently used by the IGS must be revisited to consider not only clocks but also biases. A combination of PPP-AR products from six analysis centers over a one-week period is successfully achieved, showing that alignment of phase clocks can be achieved with millimeter precision thanks to the integer properties of the clocks. In the positioning domain, PPP-AR solutions for all products show improved longitude estimates of daily static positions by nearly 60% over float solutions. The combined products generally provide equivalent or better results than individual analysis center contributions, for both static and kinematic solutions.

Keywords GNSS · IGS · Precise point positioning (PPP) · Ambiguity resolution · Satellite clock combination · Observable-specific biases

1 Introduction

The International GNSS Service (IGS) (Johnston et al. 2017) started combining GPS satellite orbits from analysis centers in 1993 and launched a combined product the following year (Beutler et al. 1995). This exercise not only allowed insights into the processing strategies of analysis centers, but generally led to a more reliable and precise solution for users. A combination of satellite clock corrections was followed and was later modified to account for the improved quality of the orbits (Kouba and Springer 2001).

The growing network of ground stations contributing to the IGS, along with refinements in processing strategies, significantly improved the quality of satellite orbits and clock corrections. This advancement in turn enabled the technique of precise point positioning (PPP), allowing a single receiver to achieve millimeter-level positioning for daily static solutions (Zumberge et al. 1997; Kouba and Héroux 2001). PPP soon became a useful alternative to differential processing, especially in remote areas where local base stations are not accessible.

In contrast to short-baseline differential solutions, PPP calls for long observation sessions to obtain an accurate solution since all error sources require either careful modeling or estimation. Furthermore, the presence of unmodeled satellite and receiver biases prevented isolating carrier-phase ambiguities as integer values (Gabor 1999). This constraint spurred a significant effort by the GNSS community to better understand these biases, and

✉ Simon Banville
simon.banville@canada.ca

1 Canadian Geodetic Survey, Natural Resources Canada, Ottawa, Canada

2 GNSS Research Center, Wuhan University, Wuhan, China

3 Collecte Localisation Satellites, Ramonville-Saint-Agne, France

4 Swisstopo/AIUB, Center for Orbit Determination in Europe, Bern, Switzerland

5 European Space Agency / European Space Operation Centre, Darmstadt, Germany

6 Graz University of Technology, Graz, Austria

techniques for PPP with ambiguity resolution (PPP-AR) subsequently emerged.

Analysis centers of the IGS have developed different approaches to achieve PPP-AR, including the computation of uncalibrated phase delays (Ge et al. 2008) and the estimation of "integer" clocks (Laurichesse et al. 2009; Collins et al. 2010). These techniques have significantly matured over the years, and research has demonstrated connections between the various models in use (Teunissen and Khodabandeh 2015). Initial efforts have also shown that a combination of these products preserving the integer characteristics of ambiguities at the user end is possible (Seepersad et al. 2016).

Even though access to publicly available PPP-AR products is still limited, several analysis centers are generating such products for internal purposes. In an effort to move the IGS toward the adoption of combined satellite clock products supporting PPP-AR, a working group has been created at the 2018 IGS Workshop held in Wuhan, China. An objective of the working group is to demonstrate the interoperability of the products generated by analysis centers. To achieve this goal, this paper first looks at a recent initiative within the IGS encouraging analysis centers to provide observable-specific signal biases along with their satellite orbits and clock corrections. The next section explains how common PPP-AR models can be cast into such a representation. The concepts of a satellite clock and bias combination are then described, followed by experimental results and PPP-AR solutions.

2 Satellite clocks and observable-specific signal biases

All satellite clock corrections, including those estimated by IGS analysis centers, are determined with respect to a timing reference, typically a single or an ensemble of hydrogen maser atomic clock(s). A stable reference is preferred to ensure that clock corrections exhibit the characteristics of the underlying oscillator and allow atomic clocks to be interpolated (or extrapolated) as precisely as possible. A convention currently adopted by the IGS is the use of the ionosphere-free linear combination of the GPS C1W and C2W code observables as a reference signal, where observable identification follows RINEX 3 conventions (Gurtner and Estey 2018). Therefore, satellite clock corrections contain satellite equipment delays (or biases) associated with these observables. Following these considerations, it can be shown that dual-frequency satellite clock corrections provided by an analysis center, denoted here by an overbar symbol, can be modeled as:

$$\overline{\mathrm{d}t}^{j} = \mathrm{d}t^{j} - \Delta t - \left(\alpha_{\mathrm{IF}} b^{j}_{\mathrm{C1W}} + \beta_{\mathrm{IF}} b^{j}_{\mathrm{C2W}}\right) \tag{1}$$

where superscript j identifies a satellite. The satellite clock offset with respect to GPS time is given by $\mathrm{d}t$, the analysis center timing offset is described by Δt, and the code biases on the C1W and C2W signals are represented by b. All quantities are expressed in units of meters. The sign convention for biases follows the Bias-SINEX format V1.00 which states that bias corrections should be subtracted from observations (Schaer 2016). The frequency-dependent ionosphere-free coefficients are defined as:

$$\alpha_{\mathrm{IF}} = \frac{f_1^2}{f_1^2 - f_2^2} \tag{2}$$

$$\beta_* = 1 - \alpha_* \tag{3}$$

where f_i is the frequency on the L_i carrier. The star symbol indicates that Eq. 3 is valid for other linear combinations included in this paper.

Some analysis centers are also estimating C1W–C2W differential code bias (DCB) corrections (Schaer 1999). These quantities are required to ensure consistency for single-frequency users. In the following derivations, we will restrict our analysis to the C1C, C1W and C2W signals, although the concepts can be extended to include any frequencies or modulations. From the three selected signals, two independent DCB corrections can be defined, specifically for C1W–C2W and C1W–C1C:

$$\mathrm{DCB}_{\mathrm{C1W,C2W}} = b^{j}_{\mathrm{C1W}} - b^{j}_{\mathrm{C2W}} \tag{4}$$

$$\mathrm{DCB}_{\mathrm{C1W,C1C}} = b^{j}_{\mathrm{C1W}} - b^{j}_{\mathrm{C1C}} \tag{5}$$

It is the user's responsibility to apply these DCBs to their observations to ensure consistency with the satellite clock corrections (Collins et al. 2005). Equivalently, observable-specific clock corrections can be determined by a user:

$$\overline{\mathrm{d}t}^{j} - \beta_{\mathrm{IF}}\mathrm{DCB}_{\mathrm{C1W,C2W}} = \mathrm{d}t^{j} - \Delta t - b^{j}_{\mathrm{C1W}} \tag{6}$$

$$\overline{\mathrm{d}t}^{j} + \alpha_{\mathrm{IF}}\mathrm{DCB}_{\mathrm{C1W,C2W}} = \mathrm{d}t^{j} - \Delta t - b^{j}_{\mathrm{C2W}} \tag{7}$$

$$\overline{\mathrm{d}t}^{j} - \beta_{\mathrm{IF}}\mathrm{DCB}_{\mathrm{C1W,C2W}} + \mathrm{DCB}_{\mathrm{C1W,C1C}} = \mathrm{d}t^{j} - \Delta t - b^{j}_{\mathrm{C1C}} \tag{8}$$

As shown in Eq. 8, a single-frequency receiver tracking the C1C signal can use the satellite clock correction defined in Eq. 1 along with two DCB corrections to correct for both the satellite clock and the C1C bias. It is therefore critical that users know which reference observables are used in the network solution to properly apply DCB corrections. If an analysis center would choose to use the C1C and C2W

observables to compute satellite clock corrections, Eqs. 6–8 would need to be modified accordingly.

A more convenient approach to ensure consistency between clocks and biases is for analysis centers to provide observable-specific signal bias (OSB) corrections (Villiger et al. 2019), which is now possible thanks to the Bias-SINEX format. Let us represent the estimated quantities of Eqs. 1, 4 and 5 in matrix form as a function of OSBs:

$$\begin{bmatrix} \overline{\mathrm{d}t}^{j} \\ \mathrm{DCB}_{\mathrm{C1W,C2W}} \\ \mathrm{DCB}_{\mathrm{C1W,C1C}} \\ 0 \end{bmatrix} = \begin{bmatrix} 1 & -\alpha_{\mathrm{IF}} & -\beta_{\mathrm{IF}} & 0 \\ 0 & 1 & -1 & 0 \\ 0 & 1 & 0 & -1 \\ 0 & \alpha_{\mathrm{IF}} & \beta_{\mathrm{IF}} & 0 \end{bmatrix} \begin{bmatrix} \mathrm{d}t^{j} - \Delta t \\ \bar{b}^{j}_{\mathrm{C1W}} \\ \bar{b}^{j}_{\mathrm{C2W}} \\ \bar{b}^{j}_{\mathrm{C1C}} \end{bmatrix} \tag{9}$$

The last line is a datum constraint to provide a consistent system of equations: It implies that dual-frequency users tracking the C1W and C2W signals do not need additional corrections for consistency since these biases are included in the satellite clock corrections. Solving this system leads to the sought-for OSBs:

$$\begin{aligned} \bar{b}^{j}_{\mathrm{C1W}} &= \beta_{\mathrm{IF}} \mathrm{DCB}_{\mathrm{C1W,C2W}} \\ &= \beta_{\mathrm{IF}} \left(b^{j}_{\mathrm{C1W}} - b^{j}_{\mathrm{C2W}} \right) \end{aligned} \tag{10}$$

$$\begin{aligned} \bar{b}^{j}_{\mathrm{C2W}} &= -\alpha_{\mathrm{IF}} \mathrm{DCB}_{\mathrm{C1W,C2W}} \\ &= -\alpha_{\mathrm{IF}} \left(b^{j}_{\mathrm{C1W}} - b^{j}_{\mathrm{C2W}} \right) \end{aligned} \tag{11}$$

$$\begin{aligned} \bar{b}^{j}_{\mathrm{C1C}} &= \beta_{\mathrm{IF}} \mathrm{DCB}_{\mathrm{C1W,C2W}} - \mathrm{DCB}_{\mathrm{C1W,C1C}} \\ &= b^{j}_{\mathrm{C1C}} - \alpha_{\mathrm{IF}} b^{j}_{\mathrm{C1W}} - \beta_{\mathrm{IF}} b^{j}_{\mathrm{C2W}} \end{aligned} \tag{12}$$

In the above equations, the first line represents the closed-form solution of Eq. 9, while the second line expresses the estimated biases as a function of the individual biases. The overbar symbol emphasizes that we are not obtaining an absolute value for these quantities. Rather, OSBs are linear combinations of individual biases and subscripts indicate to which observables they are applied, not their physical content. The key aspect of this transformation is that an analysis center can provide a consistent set of corrections (clocks and biases) to be applied on a signal-by-signal basis at the user end. With this approach, users do not need to be concerned about the reference observables or the processing strategy utilized by the analysis center.

3 PPP-AR corrections

While the IGS sets guidelines/standards for GNSS products, each analysis center is allowed freedom in developing innovative solutions. As a result, the estimation of satellite clock corrections and biases enabling PPP-AR at the user end is performed using various approaches by analysis centers. Since the processing strategy used by an analysis center impacts the definition of OSBs, four strategies are considered herein, depending on the observables used and the type of estimable bias parameters set up in the adjustment. These strategies are summarized in Table 1 and are detailed below.

Table 1 Categorization of processing strategies for generating PPP-AR products

Strategy	Observables	Estimable bias parameters
1	Ionosphere-free linear combinations	Phase
2	Ionosphere-free linear combinations	Code
3	Uncombined observations	Phase
4	Uncombined observations	Code

For simplicity, the following derivations assume constant OSBs over a day. From previous analyses, GPS biases on the L1 and L2 frequencies are generally sufficiently stable to support this assumption. Nevertheless, the transformations provided below are valid regardless of the stability of the biases and can be easily extended to account for multiple frequencies and modulations.

3.1 Uncalibrated phase delays

In strategy 1, phase biases required for PPP-AR can be derived from the standard solution produced by some analysis centers. Ambiguity resolution on the network side is achieved on the double-differenced level, i.e., by forming ambiguity differences between pairs of stations and satellites (Blewitt 1989). This procedure cancels receiver and satellite biases, thereby isolating ambiguities as integer quantities. When double-differenced ambiguities are fixed to integers, the difference between the fractional parts of two ambiguities tracked at a station gives the between-satellite uncalibrated phase delay (UPD) (Ge et al. 2008; Geng et al. 2012). Applying a zero-mean constraint or fixing a UPD to zero allows obtaining undifferenced UPDs. A user applying these UPD corrections would thus be able to recover ambiguities with the same integer properties as on the network side.

This methodology is often applied first to the Melbourne–Wübbena combination to obtain the widelane (WL) UPDs. The integer widelane ambiguities are then introduced into the ionosphere-free combination of carrier phases to isolate the L1 ambiguity from which the ionosphere-free (IF) UPDs can be derived. Assuming a common clock between the carrier-phase and code observations, the ionosphere-free UPDs effectively represent the difference between the ionosphere-free phase and code

biases. These two additional quantities can be used to augment the system of Eq. 9 as:

$$\begin{bmatrix} \overline{\mathrm{d}t}^{j} \\ \mathrm{DCB}_{\mathrm{C1W,C2W}} \\ \mathrm{DCB}_{\mathrm{C1W,C1C}} \\ 0 \\ \mathrm{UPD}_{\mathrm{WL}} \\ \mathrm{UPD}_{\mathrm{IF}} \end{bmatrix} = \begin{bmatrix} 1 & -\alpha_{\mathrm{IF}} & -\beta_{\mathrm{IF}} & 0 & 0 & 0 \\ 0 & 1 & -1 & 0 & 0 & 0 \\ 0 & 1 & 0 & -1 & 0 & 0 \\ 0 & \alpha_{\mathrm{IF}} & \beta_{\mathrm{IF}} & 0 & 0 & 0 \\ 0 & -\alpha_{\mathrm{NL}} & -\beta_{\mathrm{NL}} & 0 & \alpha_{\mathrm{WL}} & \beta_{\mathrm{WL}} \\ 0 & \alpha_{\mathrm{IF}} & \beta_{\mathrm{IF}} & 0 & -\alpha_{\mathrm{IF}} & -\beta_{\mathrm{IF}} \end{bmatrix} \begin{bmatrix} \mathrm{d}t^{j} - \Delta t \\ \bar{b}^{j}_{\mathrm{C1W}} \\ \bar{b}^{j}_{\mathrm{C2W}} \\ \bar{b}^{j}_{\mathrm{C1C}} \\ \bar{b}^{j}_{\mathrm{L1}} \\ \bar{b}^{j}_{\mathrm{L2}} \end{bmatrix} \tag{13}$$

where the widelane and narrowlane (NL) coefficients contained in the Melbourne–Wübbena combination are defined as:

$$\alpha_{\mathrm{WL}} = \frac{f_1}{f_1 - f_2} \tag{14}$$

$$\alpha_{\mathrm{NL}} = \frac{f_1}{f_1 + f_2} \tag{15}$$

and the β coefficients are obtained from Eq. 3. The two estimated UPDs enable the computation of phase biases on L1 and L2. Note that no modulations are specified here for carrier-phase signals since it is assumed that all modulations are aligned. The system of Eq. 13 will not alter the definition of the satellite clocks of Eq. 1 and code biases already obtained in Eqs. 10–12 because of the null subspace with those parameters. The observable-specific phase biases are given in closed form as:

$$\begin{aligned} \bar{b}^{j}_{\mathrm{L1}} &= \frac{\left[-f_2 \mathrm{UPD}_{\mathrm{WL}} - \left(f_1 + f_2\right)\mathrm{UPD}_{\mathrm{IF}}\right]}{f_1} - \beta_{\mathrm{IF}} \mathrm{DCB}_{\mathrm{C1W,C2W}} \\ &= b^{j}_{\mathrm{L1}} - \alpha_{\mathrm{IF}} b^{j}_{\mathrm{C1W}} - \beta_{\mathrm{IF}} b^{j}_{\mathrm{C2W}} \end{aligned} \tag{16}$$

$$\begin{aligned} \bar{b}^{j}_{\mathrm{L2}} &= \frac{\left[-f_1 \mathrm{UPD}_{\mathrm{WL}} - \left(f_1 + f_2\right)\mathrm{UPD}_{\mathrm{IF}}\right]}{f_2} + \alpha_{\mathrm{IF}} \mathrm{DCB}_{\mathrm{C1W,C2W}} \\ &= b^{j}_{\mathrm{L2}} - \alpha_{\mathrm{IF}} b^{j}_{\mathrm{C1W}} - \beta_{\mathrm{IF}} b^{j}_{\mathrm{C2W}} \end{aligned} \tag{17}$$

These phase biases, along with satellite clock and code bias corrections, effectively enable ambiguity resolution at the user end. The fact that these phase biases are functionally dependent on the code biases is a consequence of the use of a clock parameter containing code biases. Therefore, any a priori physical or stochastic assumption made about the code biases is imposed on the notional phase bias.

3.2 Integer clocks

While determining UPDs is typically a separate process from clock estimation, a second implementation of strategy 1 consists of estimating both clocks and ionosphere-free phase biases simultaneously in an adjustment. The clock parameters obtained from this process are often referred to as "integer clocks." To avoid singularities introduced by the additional unknown bias parameters, an ambiguity datum must be introduced (Collins et al. 2010). This datum is defined by fixing, a priori, a set of independent ambiguities to arbitrary integer values. These datum ambiguities propagate into the estimated parameters and lead to undifferenced ambiguities having integer properties (Odijk et al. 2016). While UPDs are typically contained within a fraction of a cycle, the numerical value of phase biases estimated using this implementation will depend on the a priori values for the datum ambiguities. The transformation from ionosphere-free phase biases to OSBs is again performed using Eq. 13 and provides biases that are compatible with UPDs in terms of definition.

Setting up ionosphere-free code instead of phase biases in the adjustment leads to what is often referred to as "phase clocks" (strategy 2). This term implies that the estimated clocks contain ionosphere-free phase biases rather than ionosphere-free code biases and that clock corrections can contain arbitrary offsets associated with datum ambiguities. In this case, the system of Eq. 13 needs to be adapted in the following way:

$$\begin{bmatrix} \overline{\overline{\mathrm{d}t}}^{j} \\ \mathrm{DCB}_{\mathrm{C1W,C2W}} \\ \mathrm{DCB}_{\mathrm{C1W,C1C}} \\ 0 \\ \mathrm{UPD}_{\mathrm{WL}} \\ b^{j}_{\mathrm{IF}} \end{bmatrix} = \begin{bmatrix} 1 & 0 & 0 & 0 & -\alpha_{\mathrm{IF}} & -\beta_{\mathrm{IF}} \\ 0 & 1 & -1 & 0 & 0 & 0 \\ 0 & 1 & 0 & -1 & 0 & 0 \\ 0 & 0 & 0 & 0 & \alpha_{\mathrm{IF}} & \beta_{\mathrm{IF}} \\ 0 & -\alpha_{\mathrm{NL}} & -\beta_{\mathrm{NL}} & 0 & \alpha_{\mathrm{WL}} & \beta_{\mathrm{WL}} \\ 0 & -\alpha_{\mathrm{IF}} & -\beta_{\mathrm{IF}} & 0 & \alpha_{\mathrm{IF}} & \beta_{\mathrm{IF}} \end{bmatrix} \begin{bmatrix} \mathrm{d}t^{j} - \Delta t \\ \overline{\overline{b}}^{j}_{\mathrm{C1W}} \\ \overline{\overline{b}}^{j}_{\mathrm{C2W}} \\ \overline{\overline{b}}^{j}_{\mathrm{C1C}} \\ \overline{\overline{b}}^{j}_{\mathrm{L1}} \\ \overline{\overline{b}}^{j}_{\mathrm{L2}} \end{bmatrix} \tag{18}$$

where the datum constraint (line 4) is now applied to the phase biases. The ionosphere-free code biases $\left(b^{j}_{\mathrm{IF}}\right)$ correspond to the offset between the "code clocks" of Eq. 1 and the phase clocks. The resulting satellite clock and OSBs are:

$$\overline{\overline{\mathrm{d}t}}^{j} = \mathrm{d}t^{j} - \Delta t - \left(\alpha_{\mathrm{IF}} b^{j}_{\mathrm{L1}} + \beta_{\mathrm{IF}} b^{j}_{\mathrm{L2}}\right) \tag{19}$$

$$\begin{aligned} \overline{\overline{b}}^{j}_{\mathrm{C1W}} &= \beta_{\mathrm{IF}} \mathrm{DCB}_{\mathrm{C1W,C2W}} - b^{j}_{\mathrm{IF}} \\ &= b^{j}_{\mathrm{C1W}} - \alpha_{\mathrm{IF}} b^{j}_{\mathrm{L1}} - \beta_{\mathrm{IF}} b^{j}_{\mathrm{L2}} \end{aligned} \tag{20}$$

$$\begin{aligned} \overline{\overline{b}}^{j}_{\mathrm{C2W}} &= -\alpha_{\mathrm{IF}} \mathrm{DCB}_{\mathrm{C1W,C2W}} - b^{j}_{\mathrm{IF}} \\ &= b^{j}_{\mathrm{C2W}} - \alpha_{\mathrm{IF}} b^{j}_{\mathrm{L1}} - \beta_{\mathrm{IF}} b^{j}_{\mathrm{L2}} \end{aligned} \tag{21}$$

$$\begin{aligned}\overline{\overline{b}}^{j}_{\mathrm{C1C}} &= \beta_{\mathrm{IF}}\mathrm{DCB}_{\mathrm{C1W,C2W}} - \mathrm{DCB}_{\mathrm{C1W,C1C}} - b^{j}_{\mathrm{IF}} \\ &= b^{j}_{\mathrm{C1C}} - \alpha_{\mathrm{IF}} b^{j}_{\mathrm{L1}} - \beta_{\mathrm{IF}} b^{j}_{\mathrm{L2}}\end{aligned} \tag{22}$$

$$\begin{aligned}\overline{\overline{b}}^{j}_{\mathrm{L1}} &= \frac{-f_2\left(\mathrm{UPD}_{\mathrm{WL}} - b^{j}_{\mathrm{IF}}\right)}{f_1} - \beta_{\mathrm{IF}}\mathrm{DCB}_{\mathrm{C1W,C2W}} \\ &= \beta_{\mathrm{IF}}\left(b^{j}_{L1} - b^{j}_{L2}\right)\end{aligned} \tag{23}$$

$$\begin{aligned}\overline{\overline{b}}^{j}_{\mathrm{L2}} &= \frac{-f_1\left(\mathrm{UPD}_{\mathrm{WL}} - b^{j}_{\mathrm{IF}}\right)}{f_2} + \alpha_{\mathrm{IF}}\mathrm{DCB}_{\mathrm{C1W,C2W}} \\ &= -\alpha_{\mathrm{IF}}\left(b^{j}_{\mathrm{L1}} - b^{j}_{\mathrm{L2}}\right)\end{aligned} \tag{24}$$

In the above equations, the double overbar symbol is used to differentiate these quantities from the ones derived from Eq. 13. Hence, whether a phase clock or a code clock is defined impacts the definition of the associated biases. As a result, when biases are taken independently (without the clock corrections), compatibility cannot be guaranteed. The next section will explain how interoperability between these formulations can be achieved. But first, two additional strategies based on uncombined observations will be discussed. Using uncombined observations, OSBs are obtained directly from the adjustment and can be provided to users as is. It has been shown that the definition of satellite clocks and phase biases based on uncombined observations (strategy 3) is identical to the one obtained from the corresponding ionosphere-free formulation (Zhang et al. 2018). The same can be shown to be true for strategy 4.

4 Combination principles

Even though the definition of OSBs varies as a function of the underlying processing strategy, a fundamental property of the above transformations is that they respect the following condition:

$$\overline{\mathrm{d}t}^{j} - \bar{b}^{j}_{*} = \mathrm{d}t^{j} - \Delta t - b^{j}_{*} \tag{25}$$

This equality can be verified using all transformations derived so far; for instance, subtracting the L1 phase bias of Eq. 16 from the clock correction of Eq. 1 allows obtaining a satellite clock correction biased solely by the L1 phase bias. This result is obtained despite the fact that the L1 phase bias of Eq. 16 contains the contribution of code biases.

The above condition implies that, when clocks and biases are taken together, the true nature of the individual biases is recovered. Hence, when Eq. 25 is satisfied, interoperability between corrections from different analysis centers is ensured. It also emphasizes that clocks and biases are intimately tied and must be used together.

Equation 25 suggests that a combination of satellite clocks can be performed on a per-signal basis or by forming linear combinations of biases. To understand the principles underlying phase-clock combination, let us analyze the case of L1 phase clocks from two analysis centers (A and B) and two satellites (j and k):

$$\overline{\mathrm{d}t}^{j}_{A} - \bar{b}^{j}_{\mathrm{L1},A} = \mathrm{d}t^{j}_{\mathrm{L1}} - \Delta t_A + \lambda_1 N^{j}_{A} \tag{26}$$

$$\overline{\mathrm{d}t}^{k}_{A} - \bar{b}^{k}_{\mathrm{L1},A} = \mathrm{d}t^{k}_{\mathrm{L1}} - \Delta t_A + \lambda_1 N^{k}_{A} \tag{27}$$

$$\overline{\mathrm{d}t}^{j}_{B} - \bar{b}^{j}_{\mathrm{L1},B} = \mathrm{d}t^{j}_{\mathrm{L1}} - \Delta t_B + \lambda_1 N^{j}_{B} \tag{28}$$

$$\overline{\mathrm{d}t}^{k}_{B} - \bar{b}^{k}_{\mathrm{L1},B} = \mathrm{d}t^{k}_{\mathrm{L1}} - \Delta t_B + \lambda_1 N^{k}_{B} \tag{29}$$

where $\mathrm{d}t^{*}_{\mathrm{L1}}$ implies a combination of satellite clock and L1 phase bias. An interesting property of phase clocks is that they can be precisely aligned by shifting clocks by an integer number of wavelengths (λ) of the signal. For this purpose, an ambiguity-like term (N) is added to Eqs. 26–29. Each observable-specific clock is thus a function of the satellite clock, the analysis center timing offset and this ambiguity parameter. Based on this formulation, four equations are available for the estimation of eight parameters in the example provided. This means that four unknowns must be selected as datum parameters.

The first singularity can be eliminated by selecting the timing offset of one analysis center as the reference, say Δt_A. To preserve the integer nature of the ambiguity parameters, the remaining datum parameters must be ambiguity parameters forming a graph connecting all analysis centers and satellites (Lannes and Prieur 2013). For instance, by selecting N^{j}_{A}, N^{k}_{A} and N^{j}_{B}, the resulting fully observable system becomes:

$$\overline{\mathrm{d}t}^{j}_{A} - \bar{b}^{j}_{\mathrm{L1},A} = \overline{\mathrm{d}t}^{j}_{\mathrm{L1}} \tag{30}$$

$$\overline{\mathrm{d}t}^{k}_{A} - \bar{b}^{k}_{\mathrm{L1},A} = \overline{\mathrm{d}t}^{k}_{\mathrm{L1}} \tag{31}$$

$$\overline{\mathrm{d}t}^{j}_{B} - \bar{b}^{j}_{\mathrm{L1},B} = \overline{\mathrm{d}t}^{j}_{\mathrm{L1}} - \overline{\Delta t_B} \tag{32}$$

$$\overline{\mathrm{d}t}^{k}_{B} - \bar{b}^{k}_{\mathrm{L1},B} = \overline{\mathrm{d}t}^{k}_{\mathrm{L1}} - \overline{\Delta t_B} + \lambda_1 \bar{N}^{k}_{B} \tag{33}$$

In Eqs. 30–33, an overbar symbol was again added to the right-hand side terms to indicate that they are now be biased by datum parameters. This strategy can be extended to the

full constellation of satellites and to any number of analysis centers. By defining an appropriate set of datum constraints, all parameters can be estimated and the integer nature of the ambiguity parameters can be preserved.

While combining observable-specific clocks, like the L1 clocks defined above, is a theoretically correct approach, it is not necessarily the recommended strategy in practice. Equations 16 and 23 show that L1 phase biases are obtained from a combination of estimates: the widelane UPD, the ionosphere-free UPD (or code bias) and a DCB correction. All of these estimates are subject to errors (refer to Sect. 6 for examples), which can mask the integer nature of the ambiguity parameters. The next section explains how this issue can be circumvented.

5 Combination methodology

Since all observable-specific clock corrections determined from Eq. 25 are correlated, they should be processed simultaneously in a single adjustment considering all correlations. This leads to a complex system of equations with a large number of parameters. As a simplification to this rigorous solution, individual linear combinations of observable-specific clocks are formed and then processed using Eq. 18. This section describes the five-step methodology utilized to produce combined satellite clock corrections and OSBs.

Step 1: differential code biases

The first step consists of combining differential code bias estimates by differencing OSBs provided by each analysis center:

$$\bar{b}^j_{\mathrm{C1W}} - \bar{b}^j_{\mathrm{C2W}} = \widetilde{\mathrm{DCB}}_{\mathrm{C1W,C2W}} + \Delta t_{\mathrm{C1W,C2W}} \tag{34}$$

$$\bar{b}^j_{\mathrm{C1W}} - \bar{b}^j_{\mathrm{C1C}} = \widetilde{\mathrm{DCB}}_{\mathrm{C1W,C1C}} + \Delta t_{\mathrm{C1W,C1C}} \tag{35}$$

where the tilde symbol identifies combined estimates. Since DCBs are determined with respect to a specific constraint (e.g., a zero-mean constraint), a timing offset has been added to the right-hand side of Eqs. 34 and 35 for proper alignment of DCB corrections among analysis centers. By using one analysis center as the timing reference, or by defining a zero-mean constraint, the rank deficiency can be eliminated and combined DCB estimates can be obtained.

Step 2: Melbourne–Wübbena biases

The second step computes the Melbourne–Wübbena linear combination of estimated biases:

$$\alpha_{\mathrm{WL}}\bar{b}^j_{\mathrm{L1}} + \beta_{\mathrm{WL}}\bar{b}^j_{\mathrm{L2}} - \alpha_{\mathrm{NL}}\bar{b}^j_{\mathrm{C1W}} - \beta_{\mathrm{NL}}\bar{b}^j_{\mathrm{C2W}} = \widetilde{\mathrm{UPD}}^j_{\mathrm{WL}} + \Delta t_{\mathrm{WL}} + \lambda_{\mathrm{WL}} N^j_{\mathrm{WL}} \tag{36}$$

where

$$\lambda_{\mathrm{WL}} = \frac{c}{f_1 - f_2} \approx 86.2 \text{ cm} \tag{37}$$

and c is the speed of light. This formulation is similar to Eq. 26 and requires the datum constraints discussed in Sect. 4 to avoid singularities and maintain the integer nature of the widelane ambiguities. After a float solution is computed, additional constraints can be added to the system to fix ambiguity parameters to integers and obtain the final values for the combined Melbourne–Wübbena biases.

Step 3: ionosphere-free phase clocks

The third step is the actual clock combination using satellite clock corrections with ionosphere-free phase biases. The integer nature of ambiguity parameters in these ionosphere-free phase clocks can only be recovered when first correcting for widelane alignment differences between analysis centers. This is similar to network processing of GPS observations where resolved widelane ambiguities are introduced into ionosphere-free phase observations (Blewitt 1989). Integer widelane ambiguities $\left(\breve{N}^j_{\mathrm{WL}}\right)$ identified in step 2 are thus applied as a priori corrections to the ionosphere-free phase clocks:

$$\overline{\mathrm{d}t}^j - \alpha_{\mathrm{IF}}\bar{b}^j_{\mathrm{L1}} - \beta_{\mathrm{IF}}\bar{b}^j_{\mathrm{L2}} + \beta_{\mathrm{IF}}\lambda_2\breve{N}^j_{\mathrm{WL}} = \widetilde{\mathrm{d}t}^j - \Delta t + \lambda_{\mathrm{NL}} N^j_{\mathrm{L1}} \tag{38}$$

where

$$\lambda_{\mathrm{NL}} = \frac{c}{f_1 + f_2} \approx 10.7 \text{ cm} \tag{39}$$

Prior to the combination, the satellite clocks of each analysis center are corrected for a radial offset caused by differences in the satellite orbits (Kouba and Springer 2001). The concepts discussed in Sect. 4 can again be applied to estimate the combined satellite clock corrections, the analysis center timing offsets and the ambiguity terms. Once the latter are resolved to integer values, the combined clock corrections can be computed.

In this study, combined ionosphere-free phase clocks with resolved ambiguities are obtained using an iterative weighting scheme. In the first processing run, input clock corrections from all analysis centers are assigned identical weights. Residuals from this adjustment that exceed a pre-defined threshold are then down-weighted (Chen et al. 2017). The purpose of this process is to automatically reject outliers, and iterations

are performed until the solution has converged, i.e., no additional down-weighting is required. Based on the dispersion of the standardized residuals, a weight is then assigned to each analysis center and a last iteration is performed to yield the final estimates.

Step 4: ionosphere-free code biases

Depending on the a priori values assigned to datum ambiguities in the phase-clock solution of step 3, phase-clock estimates could be significantly offset from standard ionosphere-free code clocks following the IGS definition (see Eq. 1). It thus becomes important to compute the magnitude of these offsets to prevent code observations at the user end from containing large errors.

These offsets can be obtained by differencing the combined phase-clock estimates from step 3 and the ionosphere-free code clocks from one analysis center:

$$\left(\overline{\mathrm{d}t}_A^j - \alpha_{\mathrm{IF}}\bar{b}^j_{\mathrm{C1W},A} - \beta_{\mathrm{IF}}\bar{b}^j_{\mathrm{C2W},A}\right) - \widetilde{\mathrm{d}t}^j = \Delta t + b^j_{\mathrm{IF}} \tag{40}$$

While the timing offset is common to all satellites, the code bias $\left(b^j_{\mathrm{IF}}\right)$ is satellite dependent. Since ionosphere-free phase clocks have an integer nature, they can be shifted by an integer multiple of the wavelength without destroying their integer property. Hence, code biases can be expressed as:

$$b^j_{\mathrm{IF}} = \lambda_1 N^j_1 + \tilde{b}^j_{\mathrm{IF}} \tag{41}$$

By rounding code biases to their nearest integer multiple of the signal wavelength $\left(\breve{N}^j_1\right)$, phase clocks can be shifted to be approximately aligned to standard IGS clocks. The remaining fractional part of the code bias $\left(\tilde{b}^j_{\mathrm{IF}}\right)$ becomes the combined ionosphere-free code bias.

Step 5: transformation to OSBs

Steps 1–4 above have provided five combined estimates (identified by the tilde symbol) for the left-hand side of Eq. 18. Inverting this equation allows transforming these linear combination of biases to OSBs. If biases are estimated as time-varying quantities, Eq. 18 could be applied on a satellite-by-satellite basis at each epoch to retrieve epoch-dependent OSBs. When bias stability allows for the estimation of constant daily values for all biases (DCBs, Melbourne–Wübbena and ionosphere-free code biases), then the first line of Eqs. 20–24 can be used in closed form to compute daily OSB values.

6 Interoperability analysis

The purpose of this investigation is to analyze the interoperability of the PPP-AR products generated by IGS analysis centers. This is accomplished by performing a clock and bias combination of these products, as presented in Sect. 5, and by computing PPP-AR solutions to verify the validity of the combined products. Table 2 shows the six analysis centers which contributed products for a one-week test period, namely GPS week 2026.

6.1 Solution transformation

Since PPP-AR products are still an experimental feature for many analysis centers, the Bias-SINEX format and observable-specific signal bias formulation are not currently commonly adopted. Hence, transformations were required to convert estimated biases into OSBs. These transformations rely on knowledge of each analysis center's processing strategy. For instance, the GRG products contain daily satellite widelane biases in the RINEX clock file header. Their processing methodology for satellite clock estimation ensures that phase clocks minimize ionosphere-free code biases, making them virtually equal to zero (Loyer et al. 2012). Based on this information, and using C1W-C1C and C1W-C2W DCB values provided by CODE, OSBs were derived by inverting Eq. 18.

NRCan uses the decoupled clock model, where carrier-phase and code observables are considered to have

Table 2 Analysis centers participating in the interoperability analysis

ID	Organization	Clock interval (s)	Biases provided
COD	Center for Orbit Determination in Europe (CODE)	5	$\bar{b}^j_{\mathrm{L1}}$, $\bar{b}^j_{\mathrm{L2}}$, $\bar{b}^j_{\mathrm{C1C}}$, $\bar{b}^j_{\mathrm{C1W}}$, $\bar{b}^j_{\mathrm{C2W}}$
EMR	Natural Resources Canada (NRCan)	30	b^j_{WL} (epoch specific) b^j_{IF} (epoch specific)
ESA	European Space Agency	300	$\mathrm{UPD}_{\mathrm{WL}}$, $\mathrm{UPD}_{\mathrm{IF}}$
GRG	Centre National d'Études Spatiales (CNES)/Collecte Localisation Satellites (CLS)	30	$\mathrm{UPD}_{\mathrm{WL}}$
TUG	Graz University of Technology	30	$\bar{b}^j_{\mathrm{L1}}$, $\bar{b}^j_{\mathrm{L2}}$, $\bar{b}^j_{\mathrm{C1C}}$, $\bar{b}^j_{\mathrm{C1W}}$, $\bar{b}^j_{\mathrm{C2W}}$
WHU	Wuhan University	30	$\bar{b}^j_{\mathrm{L1}}$, $\bar{b}^j_{\mathrm{L2}}$, $\bar{b}^j_{\mathrm{C1W}}$, $\bar{b}^j_{\mathrm{C2W}}$

different timing characteristics (Collins et al. 2010). Using ionosphere-free signals, NRCan implemented strategy 2 described in Table 1, with the feature that epoch-specific code clocks replace (constant) code biases. Since this analysis center is the only one providing time-varying biases, daily averages of biases were computed for the purpose of the combination exercise. Using these values, along with C1W-C1C and C1W-C2W DCB values from CODE, Eq. 18 could again be inverted to recover OSBs.

ESA followed the UPD approach (strategy 1) initially proposed by Ge et al. (2008) and refined by Geng et al. (2012). They provided widelane and ionosphere-free UPDs which, when complemented by C1W-C1C and C1W-C2W DCBs provided by CODE, can be transformed into OSBs using Eq. 13. Note that ESA provided satellite clock corrections at a sampling interval of 5 min, as opposed to (at least) 30 s for all other analysis centers.

Even though their processing methodologies differ, all other analysis centers directly provided OSBs and no transformation was required. CODE conditioned the clock and phase bias products in such a way that maximum consistency may be ensured not only for phase-based but also for code-supported PPP applications (Schaer et al. 2018, 2019). The CODE clock product as submitted to the IGS final combination includes high-rate clock corrections (densified at intervals of 5 s). A description of the approach utilized by Wuhan University (WHU) can be found in Geng et al. (2019). It should be noted that Graz University of Technology (TUG) is, at the moment, the only analysis center whose products are based on an uncombined formulation (strategy 3) (Strasser et al. 2018). None of the analysis centers participating in this experiment used strategy 4.

6.2 Combination results

For the seven days of GPS week 2026, the five-step combination process outlined in Sect. 5 was tested using the six solutions described above. For brevity, only the results of November 4, 2018, (week 2026, day 0) are analyzed in this section, although the conclusions are similar for all other days tested. Since satellite G04 was only processed by CODE and Wuhan University, the lack of redundancy prevented reliable identification of outliers. Therefore, this satellite is not included in the results presented.

Figure 1 shows the residuals derived from the C1W-C2W DCB combination adjustments. Residuals represent the difference between individual analysis center biases and combined biases; a single value per analysis center/satellite pair is given here since daily biases are provided. As discussed in the previous section, no C1W-C2W DCB information was provided along with the original NRCan, ESA and CNES/CLS submissions. Since the same set of C1W-C2W DCB corrections was substituted for OSB conversion in these solutions, their residuals are identical and are given for the sake of completeness. The Wuhan University solution also used such a 30-day running average of C1W-C2W DCBs provided by CODE, but the values were retrieved on a different date. Note that C1W-C2W DCBs are estimated along with total electron content parameters in the generation of global ionospheric maps. Different modeling strategies for the ionospheric parameters can thus lead to discrepancies

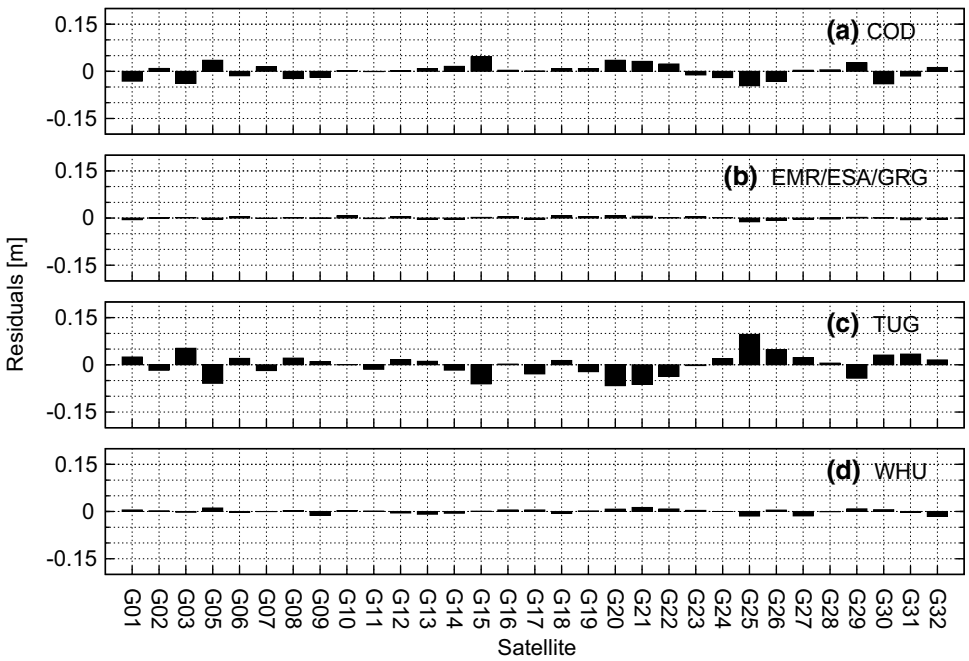

Fig. 1 Residuals from C1W-C2W DCB estimates

among analysis centers, which could explain the differences obtained by those analysis centers that considered their own C1W and C2W bias parameters (CODE and Graz University of Technology).

The C1W-C1C DCBs may be derived from the clock estimation process, as accomplished here by CODE and Graz University of Technology. Residuals from the C1W-C1C DCB adjustment are provided in Fig. 2. Again, the same running mean DCB values were used when transforming the NRCan, ESA and CNES/CLS products to OSBs. Note that Wuhan University did not provide C1C OSBs for this experiment. Differences between CODE and Graz University of Technology could be explained by the underlying network of receivers selected by each analysis center, since different manufacturers are known to have different biases for the C1C signal (Hauschild and Montenbruck 2015). Overall, the precision of all DCB estimates is at the level of a few centimeters, which indicates appropriate consistency among analysis centers.

The second step of the combination process looks into the Melbourne–Wübbena biases using the C1W and C2W code observables. Datum ambiguities were selected to remove the system's rank deficiency, and all ambiguity parameters were rounded to their nearest integers. Figure 3 depicts the residuals from this adjustment, which indicates that biases agree for the most part to within a couple of centimeters. This is remarkable given that code observations are known to be contaminated by centimeter-level receiver-dependent biases (Loyer 2015). Note that using the C1C and C2W signals to form the Melbourne–Wübbena combination would lead to different results, which would include the scaled contribution of the C1W-C1C DCB values reported above.

The next step consists of the ionosphere-free phase-clock combination. Since clocks are estimated every epoch rather than being constant over the whole day, the ambiguity datum selection needs to connect all satellite and analysis center arcs. For our purpose, an arc is defined as a continuous clock correction, free from data gaps or outliers identified by a residual rejection algorithm. In the event that a single arc is needed for all (n) satellites and (m) analysis centers, then a total of $n + m - 1$ datum ambiguities need to be defined. Currently, these datum ambiguities are selected arbitrarily based on the length of each arc. Coincidentally, most datum ambiguities for this solution were selected from the GRG solution and, as a result, the histogram of Fig. 4 contains fewer entries for this analysis center. Figure 4 shows a histogram of the fractional parts of the N_{L1} ambiguities (refer to Eq. 38) of all non-datum ambiguities. Considering the standard deviation of all ambiguity residuals indicates that ionosphere-free phase clocks can be precisely aligned to better than 0.013 narrowlane cycles (< 1.3 mm).

Once ambiguities are resolved to integer values, the final solution is computed using the iterative scheme described in Sect. 5. Figure 5 presents residuals from this adjustment, and Table 3 summarizes the standard deviation of these residuals for each analysis center. Table 3 also presents the results for the official IGS combination, as obtained from the weekly comparison report (IGS 2019). Clock solutions agree at the 1–2 mm (4–6 ps) level for most analysis center, which shows great consistency in the estimates. Even though the NRCan contribution (EMR)

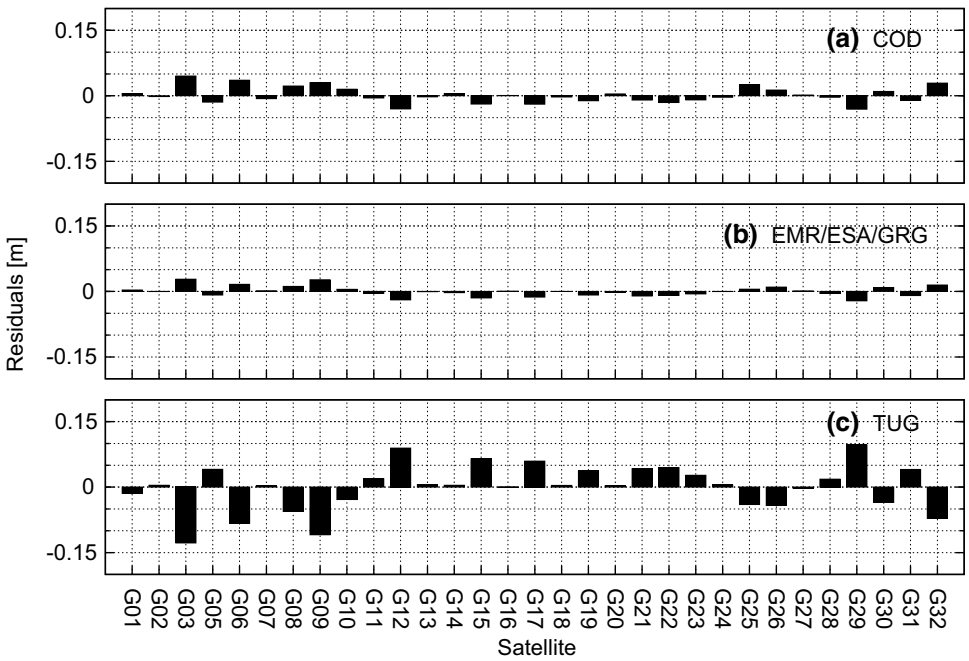

Fig. 2 Residuals from C1W-C1C DCB estimates

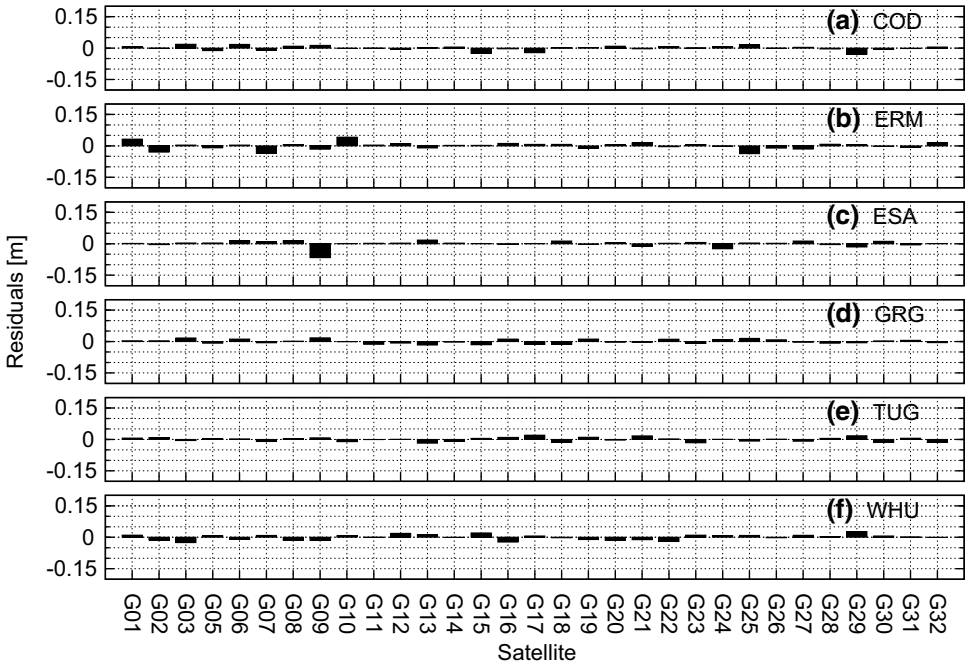

Fig. 3 Residuals from ambiguity-fixed Melbourne–Wübbena biases, referred to the C1W/C2W signals

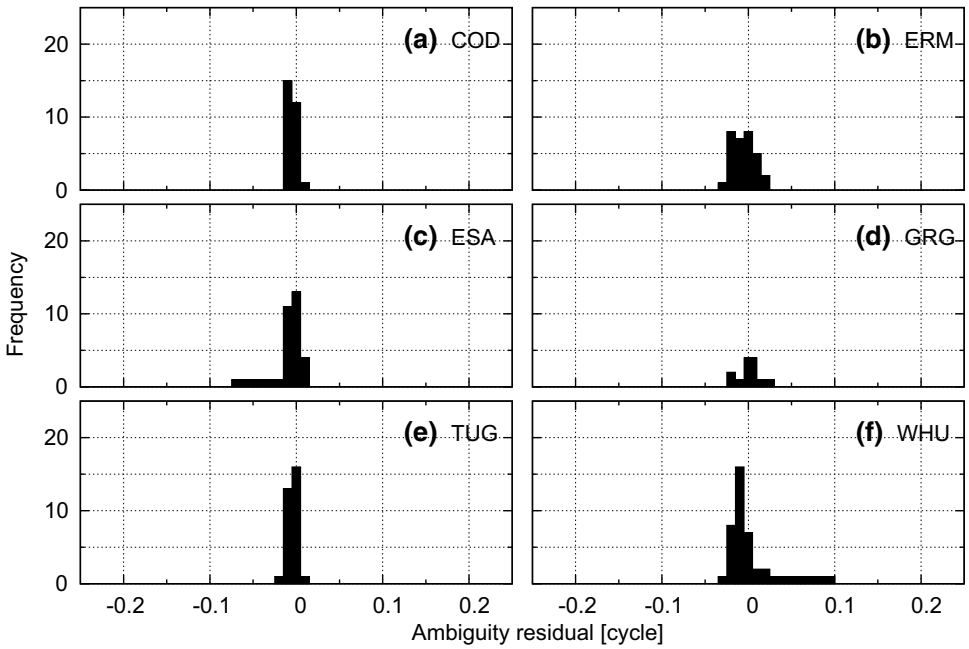

Fig. 4 Ambiguity residuals from the ionosphere-free phase clock solution

is different for both combinations, the slightly noisier results can be explained by the ambiguity float solution (IGS combination) and a forward-only filtered solution (PPP-AR combination).

At this point, the consistency of the PPP-AR products from the IGS analysis centers has been demonstrated. Step 4 of the combination aligns the ionosphere-free phase clocks to the ionosphere-free code clocks to maintain compatibility with the current definition of IGS clocks. Satellite clock corrections from various analysis centers defined as per Eq. 1 should only differ by a timing offset common to all satellites. To confirm this statement, ionosphere-free code clocks were computed for all analysis centers by adding the ionosphere-free code biases to the clock corrections provided. A combination of these ionosphere-free code clocks was then performed without the estimation of ambiguity parameters, using an equal weight for all analysis centers. The residuals from the adjustment, presented in Fig. 6, reveal the presence of satellite-dependent biases. This result shows that, even though the definition of the clock is identical for all

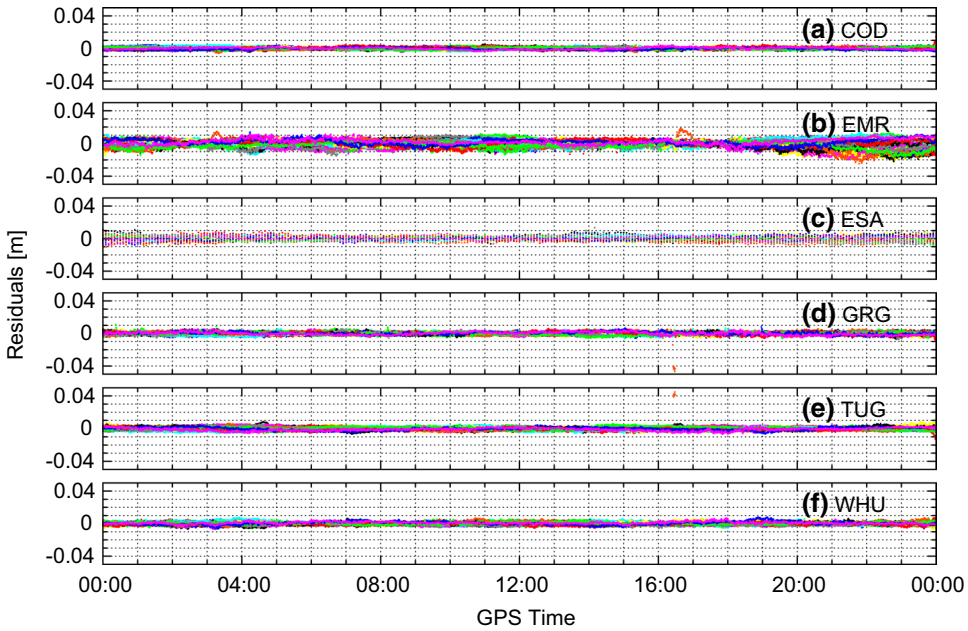

Fig. 5 Residuals from ambiguity-fixed ionosphere-free phase clocks

Table 3 Comparison of clock residuals for the IGS and PPP-AR combinations on November 4, 2018

ID	Standard deviation of clock residuals		
	IGS combination (ps) (from IGS combination report)	PPP-AR combination	
		ps	mm
COD	5	4.6	1.4
EMR[a]	16	14.5	4.4
ESA[a]	9	8.6	2.6
GRG	8	5.4	1.6
TUG	–	5.7	1.7
WHU	–	5.9	1.8

[a]Contributions are different for the IGS and PPP-AR combinations

analysis centers, the realization of the clocks is affected by unmodeled biases, likely originating from the presence of code biases in ground receivers. Based on this result and the apparent inconsistencies observed, code-phase biases from Step 4 were computed using the satellite clock corrections of a single analysis center (CODE), as described by Eqs. 40 and 41. The last step of the combination applies Eq. 18 to recover OSBs.

The main benefit of a combined product is its robustness against outliers and processing issues specific to individual analysis centers. For example, Fig. 7 shows a time series of phase clock residuals for satellite G19 on November 10, 2018, (GPS week 2026, day 6) where each color represents a different analysis center. It is clear that the satellite clock estimates provided by the analysis center pictured in red do not agree with the estimates from other analysis centers. Therefore, the combination acts as a majority voting process that downweights such estimates which should lead to an overall improved product.

7 Positioning Results

To verify the suitability of the combined satellite clock and bias products for positioning, GPS data from 209 globally distributed stations is selected over the 7-day period of GPS week 2026 (for a total of 1463 files). The station distribution is depicted in Fig. 8.

Using the NRCan PPP software, these files are processed using all products described in Table 2, in addition to the standard IGS combined clocks (labeled IGS) and the new combined PPP-AR products (labeled IAR). The IGS combined products are used in conjunction with DCB corrections provided by CODE. Four different processing schemes were tested:

1. PPP (float) static solutions
2. PPP-AR static solutions
3. PPP (float) kinematic solutions
4. PPP-AR kinematic solutions

For the static solutions, the estimated coordinates are compared against the coordinates contained in the daily IGS SINEX files, and a daily 7-parameter Helmert transformation is computed to account for reference frame alignment differences. The RMS errors for the north, east

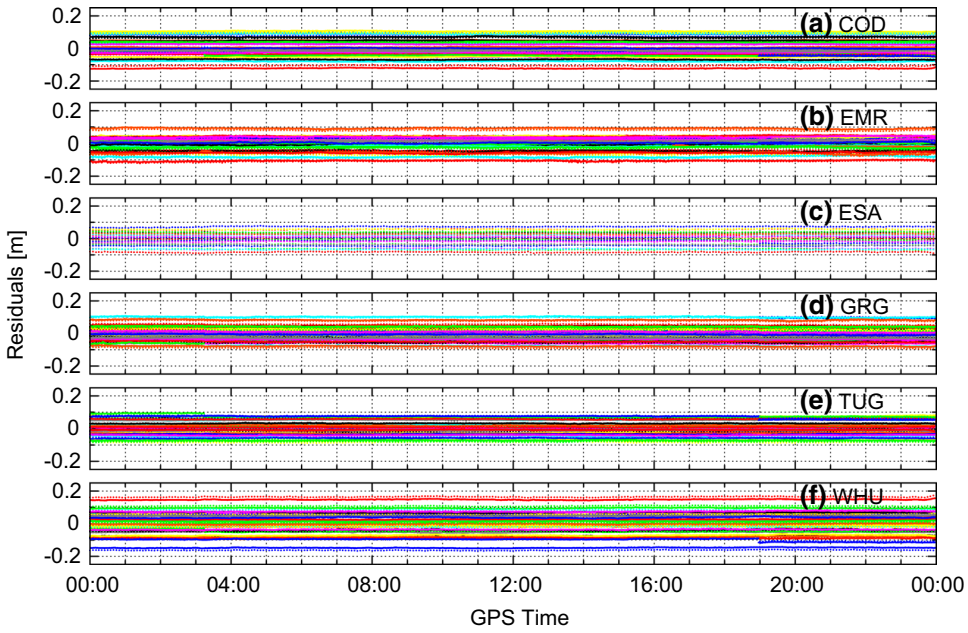

Fig. 6 Residuals from ionosphere-free code clocks without estimating ambiguity parameters

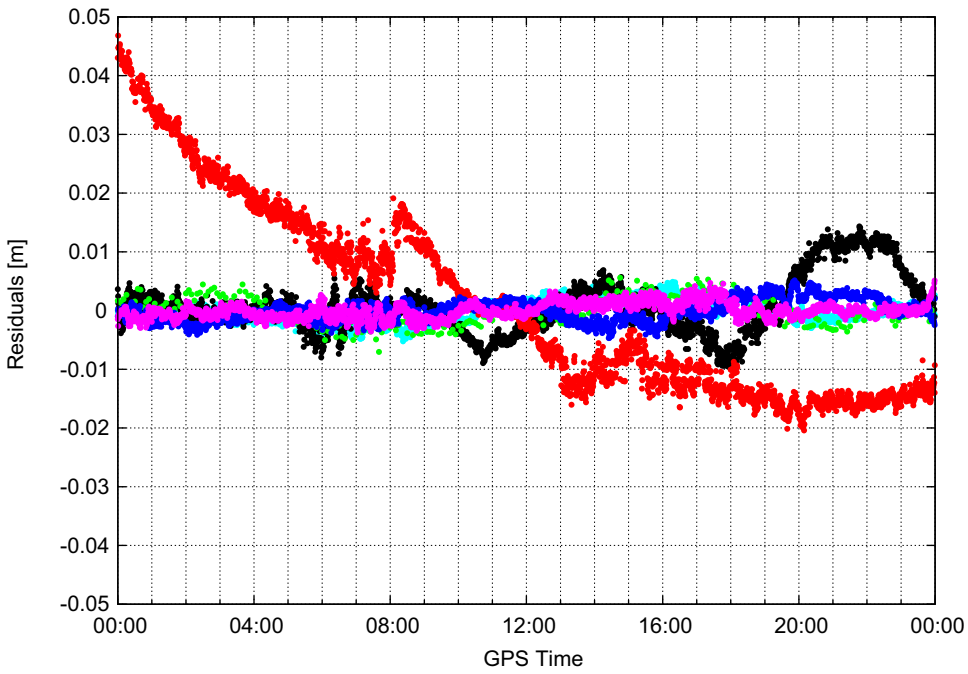

Fig. 7 Phase-clock residuals for satellite G19 on November 10, 2018. Each color represents residuals from an analysis center

and up components are then computed over the 1463 files. The results are shown in Fig. 9 for static PPP and PPP-AR solutions.

All analysis centers perform similarly, with the EMR RMS errors being slightly larger most likely due to the forward-only nature of the solution. Ambiguity resolution has a clear impact on the east (longitude) component, as expected, with a RMS reduction around 60%. Since it is not possible to recover the integer nature of the ambiguities from standard IGS clock products, this solution is not included in the bottom plot of Fig. 9. The combined PPP-AR products (IAR) perform very well, confirming the interoperability of the products.

For the second part of the analysis, data sets are processed in kinematic mode. Station coordinates are estimated independently at each epoch, while constant parameters such as carrier-phase ambiguities connect these epochs together to yield an accurate trajectory. A batch solution is implemented to mitigate convergence issues. A 30-second sampling interval is used to avoid

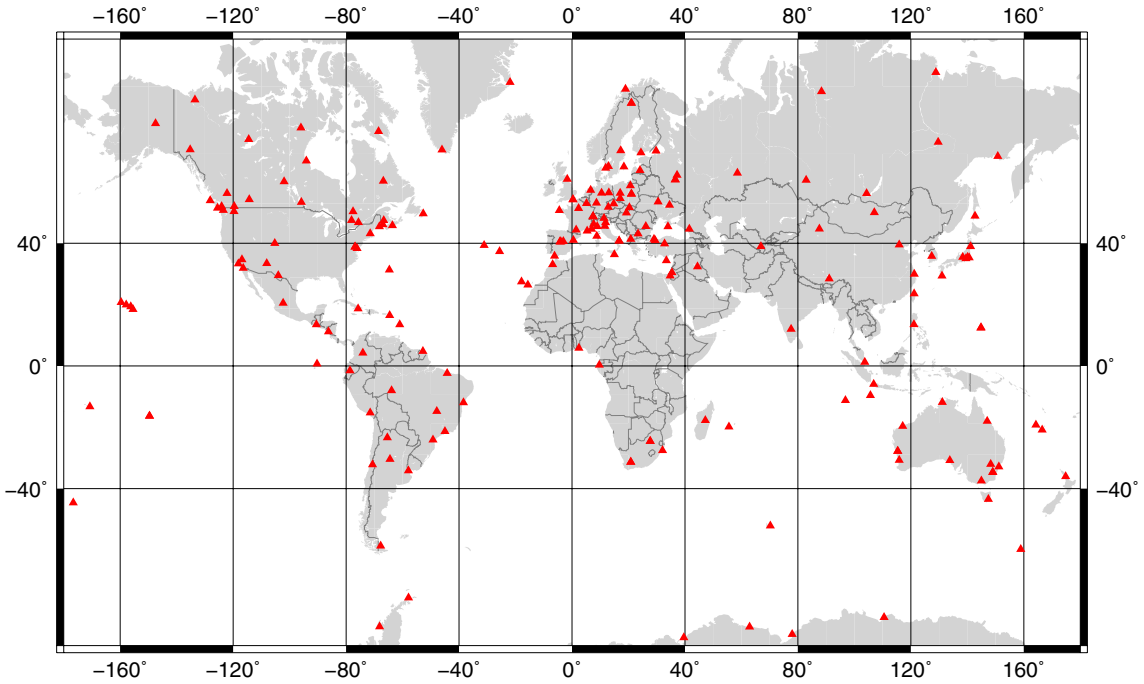

Fig. 8 Stations used in evaluating the PPP-AR products

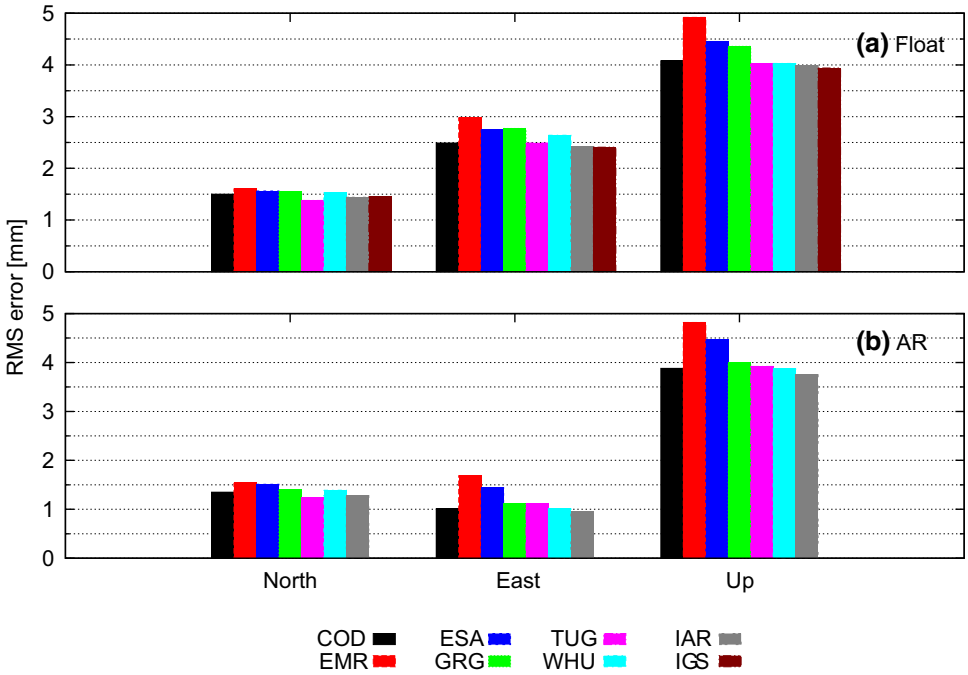

Fig. 9 RMS error of static PPP (float) and PPP-AR solutions

clock interpolation errors. In kinematic mode, data sets with signal interruptions or poor geometry can severely impact RMS errors. For this reason, the 68th percentile is reported instead of the RMS error for each analysis center. The results are presented in Fig. 10. Note that the ESA solution was not included in the kinematic evaluation since only 5-min clocks were provided. Similar conclusions as in the static case can be drawn, although the improvement in the east component is less.

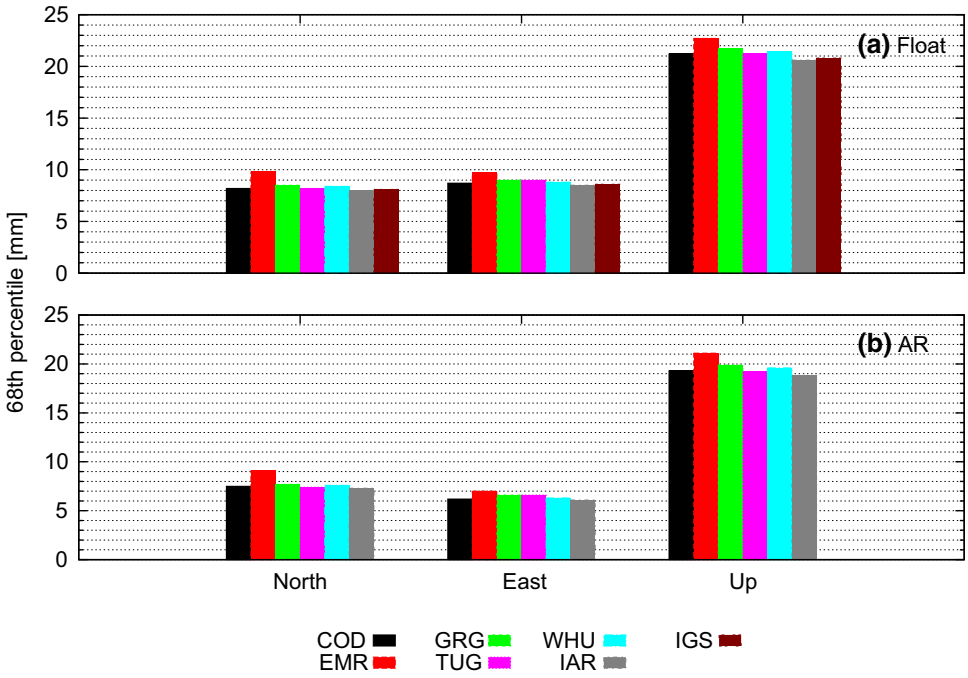

Fig. 10 68th percentile of kinematic PPP (float) and PPP-AR solutions

8 Conclusion

This paper reviewed the concept of observable-specific signal biases and explained how various combined and uncombined solutions produced by IGS analysis centers can be transformed into such a representation. Analysis centers are strongly encouraged to perform this transformation on their end to provide users with a uniform approach to ingesting PPP-AR products into their software.

A combination of PPP-AR products is more involved than simply combining satellite clock corrections. Since analysis centers can use different strategies to estimate satellite clocks and biases, these two quantities cannot be used independently. Only the joint application of clock and bias corrections offers consistency and interoperability among solutions.

An experiment conducted over a one-week period demonstrated that linear combination of biases typically have centimeter-level precision, but ionosphere-free phase clocks can be precisely aligned to within a couple of millimeters. In the positioning domain, ambiguity resolution positively impacts the east component, as demonstrated in previous studies. The combined clock and bias products perform at a similar level as products from individual analysis centers. The main benefit of using combined products is therefore the increased robustness coming from comparing several independent solutions. When ambiguity resolution is enabled, 24-hour static solutions provide RMS errors of 1.3/1.0/3.8 mm for the north, east and up components, respectively, based on a global network of 209 stations over a one-week period.

While interoperability of PPP-AR products was demonstrated, several challenges still remain before the IGS can provide combined products. For instance, inconsistencies in handling satellite eclipses create diverging clock estimates during satellite maneuvers. Exchanging satellite attitude information among analysis centers seems a way forward in mitigating this issue (Loyer et al. 2017). Furthermore, additional indicators regarding the (dis)continuity of biases must be implemented in existing data formats to ensure that users apply corrections in a consistent manner. The performance of combined products over an extended period, considering time scale alignment, must also be analyzed (Petit et al. 2015). Finally, an open issue regarding the consistency of the combined products arising from independent combinations of orbits and clock corrections must be addressed.

Acknowledgements This research was conducted under the initiative of the IGS PPP-AR working group. Thanks to Paul Collins of NRCan for providing feedback on the initial version of this paper, and to three anonymous reviewers for their comments and suggestions. This manuscript is published as Natural Resources Canada contribution number 20190080.

Author contribution S.B. proposed the concept, processed the data and wrote the manuscript. J.G., S.L., S. Schaer, T.S. and S. Strasser contributed satellite orbit, clock and bias products, provided advice and reviewed the paper.

Data availability Several satellite orbit, clock and bias products used in this study are experimental and, therefore, not publicly available. The CNES/CLS products were retrieved from ftp://cddis.gsfc.nasa.gov, while the Wuhan University phase clock/bias products can be found at ftp://igs.gnsswhu.cn/pub/whu/phasebias. CODE products enabling

PPP-AR are available for the rapid, final and MGEX analysis lines at the IGS data centers and from ftp://aiub.unibe.ch/CODE.

References

Beutler G, Kouba J, Springer T (1995) Combining the orbits of the IGS analysis centers. B Geod 69(4):200–222. https://doi.org/10.1007/BF00806733

Blewitt G (1989) Carrier-phase ambiguity resolution for the global positioning system applied to geodetic baselines up to 2000 km. J Geophys Res-Sol Ea 94(B8):10187–10203. https://doi.org/10.1029/JB094iB08p10187

Chen L, Song W, Yi W, Shi C, Lou Y, Guo H (2017) Research on a method of real-time combination of precise GPS clock corrections. GPS Solut 21(1):187–195. https://doi.org/10.1007/s10291-016-0515-3

Collins P, Gao Y, Lahaye F, Héroux P, MacLeod K, Chen K (2005) Accessing and processing real-time GPS corrections for precise point positioning—some user considerations. Proc ION GNSS 2005:1483–1491

Collins P, Bisnath S, Lahaye F, Héroux P (2010) Undifferenced GPS ambiguity resolution using the decoupled clock model and ambiguity datum fixing. Navigation 57(2):123–135

Gabor M (1999) GPS carrier phase ambiguity resolution using satellite–satellite single differences. Ph.D. Dissertation, University of Texas at Austin, USA

Ge M, Gendt G, Rothacher M, Shi C, Liu J (2008) Resolution of GPS carrier-phase ambiguities in precise point positioning (PPP) with daily observations. J Geod 82(7):389–399. https://doi.org/10.1007/s00190-007-0187-4

Geng J, Shi C, Ge M, Dodson AH, Lou Y, Zhao Q, Liu J (2012) Improving the estimation of fractional-cycle biases for ambiguity resolution in precise point positioning. J Geod 86(8):579–589. https://doi.org/10.1007/s00190-011-0537-0

Geng J, Chen X, Pan Y, Zhao Q (2019) A modified phase clock/bias model to improve PPP ambiguity resolution at Wuhan University. J Geod 93(10):2053–2067. https://doi.org/10.1007/s00190-019-01301-6

Gurtner W, Estey L (2018) RINEX: The receiver independent exchange format version 3.04. ftp://igs.org/pub/data/format/rinex304.pdf. Accessed 4 Dec 2019

Hauschild A, Montenbruck O (2015) The effect of correlator and front-end design on GNSS pseudorange biases for geodetic receivers. In: Proceedings of ION GNSS + 2015, pp 2835–2844

IGS (2019) [IGSREPORT-26247] Wk 2026 IGS Final Orbits. https://lists.igs.org/pipermail/igsreport/2018-November/026266.html. Accessed 21 May 2019

Johnston G, Riddell A, Hausler G (2017) The international GNSS service. In: Teunissen PJG, Montenbruck O (eds) Springer handbook of global navigation satellite systems, 1st edn. Springer International Publishing, Berlin, pp 967–982. https://doi.org/10.1007/978-3-319-42928-1

Kouba J, Héroux P (2001) Precise point positioning using IGS orbit and clock products. GPS Solut 5(2):12–28. https://doi.org/10.1007/PL00012883

Kouba J, Springer T (2001) New IGS station and satellite clock combination. GPS Solut 4(4):31–36. https://doi.org/10.1007/PL00012863

Lannes A, Prieur JL (2013) Calibration of the clock-phase biases of GNSS networks: the closure-ambiguity approach. J Geod 87(8):709–731. https://doi.org/10.1007/s00190-013-0641-4

Laurichesse D, Mercier F, Berthias JP, Broca P, Cerri L (2009) Integer ambiguity resolution on undifferenced GPS phase measurements and its application to PPP and satellite precise orbit determination. Navigation 56(2):135–149

Loyer S (2015) Receiver type depending part of observed satellite wide lane delays. In: IGS Workshop on GNSS Biases, 5–6 Nov, Bern, Switzerland

Loyer S, Perosanz F, Mercier F, Capdeville H, Marty JC (2012) Zero-difference GPS ambiguity resolution at CNES-CLS IGS analysis center. J Geod 86(11):991–1003. https://doi.org/10.1007/s00190-012-0559-2

Loyer S, Banville S, Perosanz F, Mercier F (2017) Disseminating GNSS satellite attitude for improved clock correction consistency. In: IGS Workshop 2017, 3–7 July, Paris, France

Odijk D, Zhang B, Khodabandeh A, Odolinski R, Teunissen PJG (2016) On the estimability of parameters in undifferenced, uncombined GNSS network and PPP-RTK user models by means of *S*-system theory. J Geod 90(1):15–44. https://doi.org/10.1007/s00190-015-0854-9

Petit G, Kanj A, Loyer S, Delporte J, Mercier F, Perosanz F (2015) $1 \times 10 - 16$ frequency transfer by GPS PPP with integer ambiguity resolution. Metrologia 52(2):301–309. https://doi.org/10.1088/0026-1394/52/2/301

Schaer S (1999) Mapping and predicting the Earth's ionosphere using the global positioning system. Ph.D. dissertation, Astronomical Institute, University of Berne, Switzerland

Schaer S (2016) Bias-SINEX format and implications for IGS bias products. In: IGS Workshop, 8–12 February, Sydney, Australia

Schaer S, Villiger A, Dach R, Prange L, Jäggi A (2018) New ambiguity-fixed IGS clock analysis products at CODE. In: IGS workshop 2018, 29 Oct–2 Nov, Wuhan, China

Schaer S, Villiger A, Arnold D, Dach R, Jäggi A, Prange L (2019) The CODE ambiguity-fixed clock and phase bias analysis products and their properties and performance. Manuscript in preparation

Seepersad G, Banville S, Collins P, Bisnath S, Lahaye F (2016) Integer satellite clock combination for precise point positioning with ambiguity resolution. Proc ION GNSS + 2016. https://doi.org/10.33012/2016.14631

Strasser S, Mayer-Gürr T, Zehentner N (2018) Processing of GNSS constellations and ground station networks using the raw observation approach. J Geod. https://doi.org/10.1007/s00190-018-1223-2

Teunissen PJG, Khodabandeh A (2015) Review and principles of PPP-RTK methods. J Geod 89(3):217–240. https://doi.org/10.1007/s00190-014-0771-3

Villiger A, Schaer S, Dach R, Prange L, Susnik A, Jäggi A (2019) Determination of GNSS pseudo-absolute code biases and their long-term combination. J Geod. https://doi.org/10.1007/s00190-019-01262-w

Zhang B, Chen Y, Yuan Y (2018) PPP-RTK based on undifferenced and uncombined observations: theoretical and practical aspects. J Geod. https://doi.org/10.1007/s00190-018-1220-5

Zumberge JF, Heflin MB, Jefferson DC, Watkins MM, Webb FH (1997) Precise point positioning for the efficient and robust analysis of GPS data from large networks. J Geophys Res-Sol Ea 102(B3):5005–5017. https://doi.org/10.1029/96JB03860